SPECTROSCOPIC STUDIES OF SOME MOLECULAR COMPLEXES OF BIOLOGICAL INTEREST

INTRODUCTION

Contemporary studies in biophysics and biochemistry stressed the importance of metal ions for the functioning of living organisms. Latest research in the field have realized the synthesis and biological characterization of compounds containing metal ions of interest due to their applications in both medicine (serve antibacterial, antitumor, gastric flow regulator) and the pharmacy (role of inhibitors, vasoconstrictors, annihilation other metals) in agronomy (used to feed pigs) and nutrition (food supplements, fortified).

The purpose of this paper is to present the synthesis and results of spectroscopic investigations performed on molecular complexes of biological interest, and finally propose a physicochemical model of metal ion coordination to a ligand of biological interest.

The paper is structured in four chapters, an introduction and conclusion. Thus, in order to address the topics studied, the following chapters are drawn:

I. Coordinative compounds of transitional metals;

II. Structural investigations of metal complexes by spectroscopic methods;

III. Raman and SERS studies of metoclopramide at different pH-values;

IV. Spectroscopic studies of manganese, copper and palladium complexes with diclofenac as ligand.

The first chapter called **Coordinative compounds of transitional metals** offers examples of compounds of transitional metals involved in the biochemical processes in living systems, highlighting their importance in the functioning of plant and animal organisms.

The second chapter entitled **Structural investigation of metal complexes by spectroscopic methods** shows how such different spectroscopic methods (FTIR, FT -Raman, UV-VIS, EPR), supplemented by chemical analyzes lead to the identification of molecular structure. Examples are offered for the interpretation of spectra and measurements of spectral parameters applied to transition metal compounds.

The third chapter entitled **Raman and SERS study of metoclopramide at different pH values** shows the structural results obtained by Raman spectroscopy applied to metoclopramide.

Metoclopramide is a gastrointestinal drug that is frequently used against nausea occurring in patients under treatment for anticancer agent.

The fourth chapter is titled **Spectroscopic studies of manganese, copper and palladium complexes with diclofenac as ligand**. Diclofenac sodium (2 - [2,6- dichlorophenilamino] phenylacetate) (L) and transition metal complexes are powerful anti-inflammatory non-steroidal drugs that have been used to alleviate pain and swelling associated with rheumatoid arthritis, osteoarthritis, spondilitele and other inflammatory conditions. New metal complexes of diclofenac with manganese, copper and palladium complexes were synthesized, which have been studied by spectroscopic methods.

The results were published in professional journals and presented at national and international scientific conferences.

CHAPTER I
COORDINATIVE COMPOUNDS OF TRANSITIONAL METALS

I.1 THE BIOLOGICAL ROLE OF TRANSITION METALS

Among the known chemical elements, 52 are identified in the composition of living matter, of which 25 are *essential* for the structure and functionality and are called *bioelements* [3,4].

Metal ions are important because they serve certain functions in the body and are involved in numerous biological processes, such as the formation and breaking of chemical bonds, charge transfer and oxygen, nitrogen fixation in the photosynthesis process, maintaining osmotic balance, enzymatic reactions, etc. They are classified according to their concentration in the human body into *essential major elements* and *essential trace elements*.

In general, the metal ions are found in living organisms or act on them in the form of complexes or are taking part in forming the complex, usually chelates. Thus, attention was paid to the process of complexation of transition metal ions' with various biomolecules. The biological activity of the complexes is dependent on the local structure around the metal ion, the type and strength of chemical bonds established.

Metal complexes of amino acids are similar in structure to the natural ones present in the body, but the release of trace elements is more efficient and is targeting the cell or tissue that needs them.

I.2 BIOINORGANIC TRANSITION METAL COMPOUNDS

Bioinorganic compounds are combinations of metal-organic; structures that are derived from any organic or inorganic. These combinations tend to maintain the identity even in solutions. Nature uses the ability to coordinate the metal ions in order to form or to stabilize the structure that is used in the interaction between biomolecules. The ions of the transitional metals, in order to form chelates with some chelatoformatori molecules, such as amino acids, peptides, carboxylic acids, have to pass through the barrier that surrounds each tissue [5].

I.3 METABOLISM OF TRACE ELEMENTS IN THE HUMAN BODY AND THE IMPORTANCE OF TRANSITION METAL -CONTAINING DRUGS

The essential elements for the proper functioning of the body are calcium, iron, magnesium, phosphorus and zinc. For the normal performance of al biological processes, another 12 elements are required. These are called *bioactive elements*, under which transitional metals, copper, cobalt, manganese, molybdenum, vanadium [9].

Introduction of trace elements required in a living organism is indicated as chelating compounds. Chelates are stable in terms of electric charge and protect the metal from chemical reactions during digestion. This property is proven for chelates complexes of bioelements with some essential or natural amino acids, such as L - histidine, L- methionine, L -aspartic acid.

In some geographical areas the soil is poor in some essential macro- and micronutrients such as Zn, Cu, Mn, Mg, making the food produced in the areas (of both vegetable and animal origin) as well as the drinking water poor in these bioions. Environmental pollution, food preservatives and stress increases the body needs of vitamins and essential macro- and micronutrients. Although the body is able to synthesize certain vitamins, it is not able to synthesize minerals, which are to be introduced through food or supplements.

I.4 LIGANDS IN TRANSITION METAL COORDINATION

Coordination compounds are usually combinations containing a central atom or ion (usually a metal) surrounded by a number of ions or neutral molecules. Electronic configuration of the transitional metals, (n -1) d^{1-10} ns^2, indicating their readiness to form compounds with a variety of ligands, such as complex combinations of cationic, anionic, mono or polycyclic and complex chelate [1, 11] .

In most *metal-bio-molecules*, metal ions bind to the molecule by forming *complex coordinative compounds*, with a high degree of covalent. In general, the metal ion bounds to the ligand though donor atoms: nitrogen, oxygen or sulfur. Transitional metals have a coordination preferred due to steric factors, for example the dimension of ligands, which determines certain geometrics of coordination [12].

Chelating is the coordination of two or more donor atoms of a ligand to a central metal atom by ciclometalare. The biochemical process is suggested by the etymology; the Greek name "chela" means pliers. As a result, the formation of a chelate coordination sphere increases the stability of complexes.

Divalent ions of transition metals bind preferentially to a given ligand. A series of stability was established: Mn < Fe < Co < Ni < **Cu** > Zn, which is called **Irwing – Williams** series. This shows that the Cu ions form the most stable complexes.

Biomolecules are built by all kinds of chemical bonds. The molecular structure is ensured by strong bonds: covalent, covalent - coordinative, ionic, while the consolidation of the structure is achieved by weaker hydrogen bonds, hydrophobic bonds and van der Waals interactions.

I.5 COORDINATION NUMBER AND GEOMETRY OF TRANSITION METAL

The coordination number N.C. represents the number of particles in close proximity to an atom, in a chemical mixture. In the complex, N.C. is the number of ligands in the immediate vicinity of the central atom or directly bonded to it.

For a given oxidation state, certain metal ions may present more coordination numbers, and for the same number of coordination, these can take several spatial geometries and configurations. In biological systems, metal ions generally form compounds with coordination numbers 4, 5, 6 and 8. The geometry of inorganic combinations, including that of coordination compounds, respects the principles of the atomic orbitals hybridization of the central metal ion theory (L.Pauling) and the principle of "repulsion of electron pairs in the valence shell" (Gillespie) [27].

CHAPTER II
STRUCTURAL INVESTIGATIONS OF METAL COMPLEXES BY SPECTROSCOPIC METHODS

II.1 VIBRATIONAL SPECTROSCOPY

The main spectroscopic methods used to investigate structural molecular complexes are vibrational IR and Raman spectroscopy, UV-VIS and ESR.

The IR and Raman spectroscopies provide information about the modes of vibration and vibration - rotation of the molecules [16]. These are complementary techniques, hence transitions that are allowed in Raman are forbidden in IR and vice versa. Since the distribution of load and energy exchange between electromagnetic radiation and the molecule is specific to each molecule, the electromagnetic field - matter interaction provides very useful information about the molecule [15].

II.1.1 INFRARED SPECTROSCOPY (IR)

An infrared spectroscopy (IR) is based on the phenomenon of absorption of infrared radiation by the molecules, having as result a change of the vibrational energy of interatomic links. Among the most important findings set out in the IR spectroscopy, is that there doesn't exist different organic compounds which have identical IR spectra. Thus, it is considered to be the most suitable method to identify the presence of functional groups in the structure of molecules of organic compounds [17].

IR spectroscopy provides both qualitative molecular information, through specific vibrational modes of molecules, and quantitative information, as shown in the Lambert -Beer law.

In practice, IR spectra can be recorded using two different spectrometers*: dispersive IR spectrophotometers and spectrometers with Fourier transformations*. Both types of IR spectrometers are based on the same operating principle: electromagnetic radiation in the IR field is emitted from a light source, is passed over the sample and then analyzed the emerging radiation whose intensity changes by interaction with organic compounds. The spectrum of the standard substance is an indication of the presence of impurities.

IR spectroscopy, samples are either used in liquid samples, when the compound is dissolved in a suitable solvent, which does not have significant absorption in the IR, or in solid samples in KBr pellet form or in the form of a suspension in paraffin oil (in sample pulverization with nujol).

A more accurate interpretation of the spectra, requires them to have a strong resolution, the substance to be is sufficiently pure, and the device to be calibrated.

For a correct interpretation of the absorption bands in the IR spectrum is necessary to identify the following: the position of the absorption band (in wave number, cm^{-1}), the shape of the band (narrow or wide), and strength of the band (high, medium, or weak).

II.1.2 RAMAN SPECTROSCOPY

Raman spectroscopy differs significantly of the IR, in that it is based on the phenomenon of inelastic scattering of photons of the incident radiation per molecule, whereby the energy changes, so the wavelength of the photon. Raman scattering occurs only if the *molecule polarizability* changes during the vibration of the molecule [19].

The great disadvantage of Raman scattering process is the fact that this is a "weak" process, because the $1/10^6$ part of the photons are scattered Raman and most photons 'suffer' elastic scattering , called scattering Raileight [19]. This is due to the effective Raman scattering, which is a very small (10_{-31} ~ 10^{-26} cm^2/ molecule) scattering, compared to the scattering for fluorescence (which is about 10^{-16} cm^2/ molecule).

II.1.3 ULTRASENZITIVĂ RAMAN SPECTROSCOPY - SERS

One of the techniques derived from the Raman investigations, that have been developed to reduce the shortcomings of techniques for investigating remains, is the *SERS - Surface Enhaced Raman Scattering*. This is the MRI method of amplification of the Raman signal on metal surfaces. Some species of molecules of biological interest, such as nucleic acids, amino acids, enzymes, proteins, and inhibitors have been successfully investigated, using the SERS technique.

This phenomenon is the electromagnetic amplification of the Raman effect, achieved by techniques to increase the effective surface. Basically molecules are attached to the surface of metal nanoparticles (gold, silver, copper) with a size between 20-300nm. This technique is very sensitive; it can reveal nanomolar concentrations. The Raman sign is although sensitive to changes in the orientation of the molecules on the metal surface. There are several types of active SERS substrates, but these two are the most commonly used: *metal colloids* (particularly, aggregated

colloids) generated by chemical and *electrode surface* which have an increased roughness by one or more cycles of reduction - electrochemical oxidation.

II.1.4. IR AND RAMAN STUDIES ON DRUGS

In 1986, T. Hirschfeld and B. Chase [25] developed techniques of processing by Fourier transformation (FT). Applying the Fourier transformation to complex functions; it produces another complex function which contains the same information as the original function, but reorganized frequencies of components. Thus, if the initial function is a time-dependent signal, the Fourier transformation decomposes the signal among the frequency and produces a spectrum of this. It turned out that this is a viable method for IR and Raman spectroscopic methods. FT -Raman spectroscopy with NIR excitation, successfully replaced Raman measurements made with conventional scanned monochromatic systems, which are using laser excitation with emission in the visible regions of the spectrum. Due to poor inelastic scattering of the Raman signal, a moderate fluorescence occurs, which can cover Raman information.

The development of FT -Raman spectrometers finds lot of benefits in many research areas, including the pharmaceutics.

A comparative analysis of the two techniques permits assessment of these methods. Data from Raman spectroscopy are complementary to those of FT-IR spectroscopy, in the sense that a complete picture of the vibrational structure is performed only by analyzing both spectra. Thus, the Raman method can be seen as a new chemical analysis or the useful solution in situations where the strips of interest are not active in the IR.

While the IR method is useful for analyzing strongly polar bands, the Raman method is useful for analyzing the non-polar or symmetrical bands. Raman spectroscopy also has several practical advantages over the IR spectroscopy. For example, the Raman spectra are recorded in the NIR or visible regions, where the glass is transparent, which makes Raman evidence to prove more viable. Thus, most of the samples can be directly studied in the laboratory bottles. A particular benefit for pharmaceutical Raman spectroscopy is the, in general, non-destructive technique that requires no sample preparation.

II.2.4 ULTRAVIOLET AND VISIBLE SPECTROSCOPY (UV -VIS)

The spectroscopy in the ultraviolet and visible light radiation is absorbed by the molecules in the field of chemicals, resulting in absorption of orbital electrons of the connection passage $\boldsymbol{\sigma}$, $\boldsymbol{\pi}$

or the non-bound **n** from a low energy state (usually the fundamental electronic state, the most populated at normal temperature) into an excited state, richer in terms of energy [15]. Since electronic transitions occur, the spectrum obtained by absorbing this radiation is called *electronic spectra.*

In the spectrum of electromagnetic radiation, the UV range is between X -ray region and the visible region, comprising wavelengths within the range of 10-400 nm. Considering the biological effects of this radiation, the UV was subdivided into three areas: *UV-A (400-320 nm)*, *UV-B (320-280 nm)* and *UV-C (280-10 nm)*. The electromagnetic radiation used in the analysis of organic compounds by this method, is in the near UV range (200-400 nm) or visible range (400-800 nm).

II.3. ELECTRON SPIN RESONANCE

The *Electron Spin Resonance* (ESR) is a branch of magnetic resonance spectroscopy based on absorption of electromagnetic radiation in the microwave range by paramagnetic molecular systems, located in a homogeneous static magnetic field. This method is known in the spectroscopy under the name of *Electron Paramagnetic Resonance* (EPR) [29].

The Electron Spin Resonance requires the presence of a kinetic momentum in the study sample. The spin angular momentum of electrons is due to the unpaired electrons pending on orbitals **p**, **d** or **f** of the gaseous atoms or molecules.

Basically, it applies a fixed frequency electromagnetic radiation ν (monochromatic radiation) and varying the magnetic field strength **B**, until it reaches the value of resonance. The ESR experiment is usually held in fixed microwave frequencies.

Transitional ion complexes are extensively studied by ESR in the presence of a number of unpaired electrons to the ions. The crystalline field is acting on the electron spin angular momentum **L**, which shows a tendency of aligning it along an axis of the crystal. The magnetic field acts on the kinetics of the spin **S** and tends to orientate it parallel with **B**. As the energy of the spin-orbit coupling is less than the contribution of the crystal field, **L** remains "frozen", hence it does not contribute to the total magnetic moment. The paramagnetic system can be described only by the electronic spin quantum number.

The main purpose of the studies on the variation parameters in EPR spectra of transitional metal complexes is to obtain information on the nature of metal - ligand bonds.

[1] Palamaru M. , A. Cecal , A. Jordan, bioinorganic chemistry and life metals; BIT Publishing, Iaşi, 1997.

[2] A. Mark A. Stanila , D. Rusu, M. Rusu , O. Cozar , L. David , Journal of Optoelectronics and Advanced Materials, 9, 3 , 2007 741.

[3] D. E. Reichert, J.S. Lewis and C.J. Anderson, Coord. Chem. Reviews, 3, 1999 184

J. H. Jeong, B. Chai, S. Y. Park, D. Kim, Bioorg. Med. Chem. Lett, 9, 1999 120.

[4] RH Garrett, CM Grisham, Biochemistry, Sanders , New York , 1995.

[5] J. Sabolović, K. Liedl; J.Inorg, Biochem, 38, 12.1999, 2764.

[6] R. Power, K.Horgan, Biological chemistry and absorption of inorganic and organic metals, European Bioscience Centre, Alltech.Inc., Dunboyne, co.meath, Ireland, 2000.

[7] G. Mark, metallic elements of modern chemistry, Technical Publishing House, Bucharest, 1993.

8. Letitia GHIZDAVU, Bioinorganic chemistry, Ed.Poliam, Cluj- Napoca, 2000.

[9] R. Lont, Copper Proteins and Copper Enzyme, CRC Press, Inc. Boca Raton, FL, Vols. 1-3, 1984.

[10] V. Masatoshi, K. Masahiro, J.Inorg. Biochem., 97, 2, 2003 240.

[11] M. Dion, M. Agler, A. John, Nutr.Cancer, 28, 1, 1997

[12] Berthon G. M. Blais, M. Piktas, J.Inorg, Biochem. 20, 2, 1984, 113.

[13] A. Gaina, Basics chemistry coordination compounds, MatrixRom, 2006.

[14] C. Cercasov, I. Baciu , A. Ciobanu, A. Nicholas, E. Popa, D. Zavoianu, D. Popovici, Organic Chemistry for improving teachers (Vol. I and II), University, Bucharest, 2001-2002.

[15] C. Batiu, I. Panea, M. Pele, A. Mark, L. David, Studia Universitatis Babes -Bolyai, Chemestry, LII, 4, 2007.

[16] A. Mark A. Stanila, O. Cozar, David L., Journal of Optoelectronics and Advanced Materials, 10, 4, 200, 730, 2007

[17] http://www.forumsci.co.il/HPLC/index.html

[18] L. David, C. Cristea, O. Cozar, L. Gaina, Identification of the molecular structure by spectroscopic methods, Cluj University Press, Cluj- Napoca, 2004

[19] S. Mager, Organic Structural Analysis, Scientific and encyclopedic edition, 1979

[20] N. Joo , M. Hossu , D. Rusu , A. Mark, M. Rusu, C. Pasca , L. David , Slovenia Chimica Acta, 54, 749, 2007.

[21] D. Rusu , A. Mark, O. Baban, M. Rusu, M. Hossu, L. David, Journal of Optoelectronics and Advanced Materials, 9, 3, 577, 2007.

[22] L. David, O. Cozar, V. Chis, C. Christmas, Electron spin resonance, Clujana University Press, Cluj, 2001

[23] I. Ursu, Electron spin resonance, Ed.Academiei RSR, Bucharest, 1965

24. http://phys.ubbcluj.ro/atomica/vchis/lab/lab.htm

[25] J.A. Weil, J.R. Bolton, J.E. Wertz, Electron Paramagnetic Resonance Pactical Theory and Applications, Wiley, New York, 1994

[26] A. Stanila, A. Mark, D. Rusu, M. Rusu, L. David, Journal of Molecular Structure, 834-836, 364, 2007.

[27] L.David, C.Crăciun, V.Chiş, O.Cozar, Electron spin resonance - Issues Paper House of Science, Cluj-Napoca, 2000, 70.

[28] T. Hirschfeld and B. Chase, " FT -Raman Spectroscopy: Development and Justification, " Appl. Spectrosc. 40, 133-137 (1986)

[29] GA Neville , HF Shurvell, Fourier transform Raman and infrared vibrational study of diazepam and four closely related 1,4- Benzodiazepines, Journal of Raman Spectroscopy, Volume 21, Issue 1, 9-19, January 1990

CHAPTER III
RAMAN AND SERS STUDY OF METOCLOPRAMIDE AT DIFFERENT PH VALUES

Metoclopramide is a gastrointestinal drug that is often used to combat the nausea that occurs for patients who are undergoing treatment with anticancer agents. Therefore, the physiological effects and physical-chemical properties of this drug are extensively studied.[1,2]

Raman scattering contains important structural information making it a powerful molecular investigation tool. When the molecules are adsorbed to rough metal surfaces the Raman cross section is enhanced several orders of magnitude and analytes in the micro-molar concentration can be investigated.[3-7] The potential to combine high sensitivity with substantial structural information content makes SERS spectroscopy a powerful tool in a variety of fields,[8-10] including biospectroscopy.[11-15]

For a proper understanding of the Raman spectra, a reliable assignment of all vibrational bands is essential. For this purpose, DFT methods, particularly hybrid functional methods[16] have evolved in the last decade to a powerful quantum chemical tool for the determination of the electronic structure of molecules. They have been shown to be successful in predicting various molecular properties, giving results of a quality comparable, or even better than highly correlated *ab initio* techniques for a substantially less computational cost. In the framework of the DFT approach, different exchange and correlation functionals are routinely used. Among these, the B3LYP combination[17,18] is the most used since it proved its ability in reproducing various molecular properties, including vibrational spectra. The combined use of B3LYP functional and standard split valence basis set 6-31G(d) has been previously shown[19-21] to provide an excellent compromise between accuracy and computational efficiency of vibrational spectra for large and medium-size molecules.

The physical processes and chemical reactions involved in biological processes are often very sensitive to the concentration of the hydrogen ions of the medium. The concentration of a drug in a tissue, at a given time, depends on the absorption, distribution and elimination of that drug.[22] The kinetics of these processes is dependent on the pK_a values of the drug. For the metoclopramide drug the pK_a values are 9.4, 1.2 and -3.1.[23] Consequently, the most present molecular species in the human organism at pH values between 2 and 8 is the protonated form presented in Fig. 1.

In this study, the conjugate acid-base forms of the metoclopramide drug were investigated by Raman spectroscopy in the solid state and in aqueous solutions and by SERS when the molecules adsorbed to the colloidal silver surface. The Raman and SERS spectra were assigned by means of DFT calculations. To the best of our knowledge, a SERS or DFT study of metoclopramide was not reported till now in the literature.

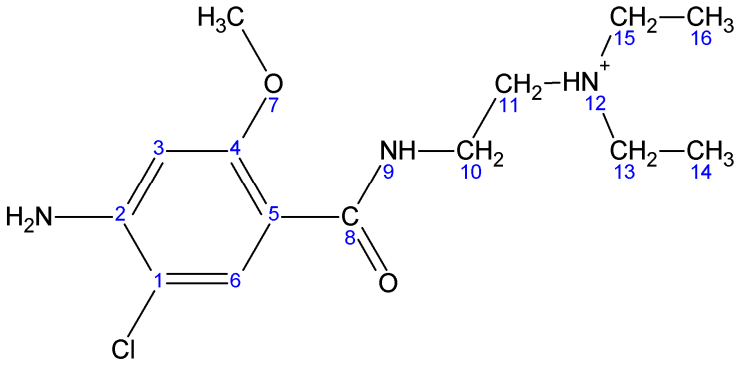

Figure 1. The protonated form of metoclopramide

EXPERIMENTAL

Chemicals

Metoclopramide hydrochloride and all the reagents were of analytical grade. The colloidal silver substrate was prepared according to the Lee-Meisel[24] procedure. Dilute hydrochloride and sodium hydroxide solutions were used to adjust the pH of the silver sol in the 3-11 pH range. When employing basic conditions, sodium chloride solution was added to the silver sol up to a final concentration of $2x10^{-3}$ M for a proper aggregation of the silver colloidal particles.

Instrumentation

Raman and SERS spectra of metoclopramide were recorded employing a micro-Raman-spectrometer (LabRam, Jobin Yvon) with an 1800 grooves/mm diffraction grating. The 514.5 nm output of a Spectra Physics argon ion laser was used as excitation wavelength and the laser power was kept below around 100 mW. The Raman and SERS spectra were collected in backscattering geometry and the spectral resolution was set to ~4 cm^{-1}. The detection system consisted of a Peltier cooled charge-coupled device (CCD) detector. Each Raman spectrum is the result of two

accumulations of 100 s exposure time. For each SERS spectrum one accumulation of 40 s exposure time was performed.

Computational details

The molecular geometry optimization and vibrational wavenumber calculations were performed with the Gaussian 03W software package[25] by using the DFT approach. The combination of the Becke's three parameter exchange functional[17] B3 with LYP correlation functional[18] was used, supplemented with the standard 6-31G(d) basis set.[26] All the calculations have been carried out with the restricted closed-shell formalism.

The vibrational wavenumbers obtained by quantum chemical calculations are typically larger than their experimental counterparts, mainly due to three cumulative effects: the anharmonic potential energy surface, the incomplete incorporation of the electron correlation and the incompleteness of the basis sets used in the calculation.[26] To compensate for these effects, empirical scaling factors in the range of 0.8 to 1.0 are commonly used to better match the experimental vibrational wavenumbers. These scaling factors depend both, on the method and basis sets, and they are determined from the mean deviation between calculated and experimental wavenumbers. From this point of view, DFT methods for which the scaling factors are approaching unity, are net superior to the conventional Hartree Fock (HF) and MP2 methods.

RESULTS AND DISCUSSION

The molecular geometry was fully optimized without any constraint with the help of analytical gradient procedure implemented within the Gaussian 03W program. The optimized geometries of the neutral and protonated metoclopramide molecules are shown in Fig. 2.

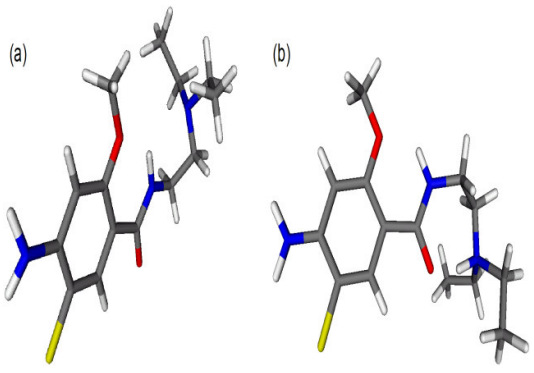

Figure 2. The optimized geometry of the neutral
(a) and protonated (b) metoclopramide molecules

The force constants were calculated by analytical differentiation algorithms, for the optimized geometry. Prior to compare the calculated vibrational wavenumbers with the experimental counterparts the former have been scaled by appropriate scaling factors recommended by Scott and Radom.[20] For the DFT method at B3LYP/6-31G(d) level, the recommended wavenumber scaling factor is 0.9614.

Vibrational mode assignments were made by visual inspection of modes animated by using the Molekel program[27, 28] by considering both, the band positions and the intensity pattern.

In Table 1 are given selected calculated geometrical parameters of metoclopramide in both, neutral and protonated forms, compared to the experimental parameters obtained for unprotonated (neutral) metoclopramide[29] and metoclopramide sulphate, where metoclopramide is in the protonated form[30].

As shown in Fig. 2 and also revealed by geometrical parameters given in Table 1, the protonated metoclopramide shows a different conformation of the diethylaminoethyl chain with respect to the unprotonated molecule.

Table 1. Selected experimental and calculated geometrical parameters of neutral and protonated molecular forms of metoclopramide (bond length in Å and angles in degrees).

Parameter	Experimental		Calculated	
	Unprotonated metoclopramide[29]	Metoclopramide sulphate[30]	Neutral	Protonated
Bond lengths				
C1C2	1.387	1.395	1.407	1.418
C2C3	1.378	1.396	1.407	1.412
C3C4	1.396	1.387	1.395	1.389
C4C5	1.407	1.412	1.415	1.423
C5C6	1.376	1.390	1.399	1.408
C6C1	1.383	1.370	1.383	1.376
C1Cl	1.734	1.748	1.767	1.756
C2N	1.365	1.376	1.382	1.357
C4O7	1.345	1.349	1.370	1.367
O7C	1.428	1.428	1.420	1.431

C5C8	1.509	1.486	1.510	1.472
C8O	1.228	1.250	1.234	1.258
C8N9	1.315	1.325	1.360	1.363
N9C10	1.459	1.456	1.449	1.457
C10C11	1.514	1.501	1.532	1.536
C11N12	1.461	1.504	1.471	1.512
N12C13	1.442	1.486	1.471	1.512
C13C14	1.503	1.510	1.530	1.525
N12C15	1.460	1.532	1.471	1.514
C15C16	1.502	1.460	1.530	1.524
O7H9	2.098	2.001	1.953	1.876
N12H9	2.709	-	2.499	-
N12H	-	0.910	-	1.067
O8H12	-	1.791	-	1.607
Bond angles				
C6C1C2	120.8	121.6	121.1	120.8
C1C2C3	117.1	117.4	117.3	117.5
C2C3C4	122.8	121.5	121.6	121.6
C3C4C5	119.2	120.3	120.7	120.6
C4C5C6	117.6	117.5	117.1	117.2
C5C6C1	122.4	121.6	122.2	122.3
C6C1Cl	119.5	119.3	119.7	119.9
C1C2N	121.1	122.2	122.1	121.6
C3C4O7	122.5	122.6	121.7	122.0
C4C5C8	126.1	126.1	128.1	126.8
C4O7C	119.0	119.5	119.7	119.7
C5C8N9	118.6	119.5	118.0	119.7
C5C8O	119.2	120.0	120.1	120.5
C8N9C10	121.9	123.4	122.1	122.4
N9C10C11	109.5	114.4	110.3	115.0
C10C11N12	113.8	112.1	112.6	112.4
C11N12C13	109.8	114.3	111.9	112.4
N12C13C14	115.7	111.1	113.1	112.6

C11N12C15	109.9	109.5	112.0	111.7
N12C15C16	112.6	113.4	113.3	112.6
C13N12C15	110.8	111.6	111.8	112.3
Dihedral angles				
C3C2C1Cl	179.1	179.3	179.0	178.6
C4C3C2N	179.0	177.8	177.1	178.6
C2C3C4O7	179.0	179.2	180.0	179.8
C3C4O7C	5.2	5.3	0.7	0.9
C6C5C8O	5.6	-5.5	3.1	-2.6
C6C5C8N9	174.2	173.3	176.2	176.3
C5C8N9C10	-177.7	174.7	-178.9	165.0
C8N9C10C11	-175.3	73.7	-146.5	75.0
N9C10C11N12	-71.1	-78.0	-54.3	-76.0
C10C11N12C13	-81.0	150.6	-78.6	149.9
C11N12C13C14	170.6	-73.8	154.7	-76.4
C10C11N12C15	156.9	-83.8	154.9	-82.8
C11N12C15C16	-74.3	159.6	-76.8	156.4

The most important differences between the geometries of the unprotonated and protonated metoclopramide are noted for the dihedral angles involving the atoms in the diethylaminoethyl chain. As shown in Table 2, these dihedral angles are qualitatively and quantitatively very well reproduced by theoretical calculations. The new conformation of the protonated metoclopramide is favored by a supplementary hydrogen bond which is realized for this form due to the rotation of the diethylaminoethyl chain around the N9-C10 bond. The C8N9C10C11 dihedral angle changes from -146.5^{o} to 75.0^{o} (calculated values), in perfect agreement with the experimental values corresponding to the unprotonated and protonated form, respectively. Also, the C10C11N12C13 dihedral angle is changing from -78.6^{o} for the unprotonated form to 149.9^{o} for the protonated form leading to the formation of the N12H…OC8 intermolecular hydrogen bond, while the N9H…O7 hydrogen bond is preserved for both, unprotonated and protonated forms. The calculated value of the length of this new bond (1.607 Å) is in good agreement with the experimental value found for the protonated form in the metoclopramide and, as seen in Table 1, it suggests a stronger hydrogen bond than the N9H…O7 hydrogen bond realized also in the unprotonated form of metoclopramide.

Moreover, from Table 1 it can also be seen that the theoretical values for the N9H…O7 intermolecular hydrogen bond suggest that it becomes stronger in the protonated form.

Overall, the trend of the bond lengths when passing from the unprotonated to the protonated form is well reproduced by theory. Some exceptions are seen for the C1Cl, C2N, C4O7, O7C, N9C10 and C13C14 bond distances.

The Raman spectrum of metoclopramide hydrochloride powder is presented in Fig. 3.

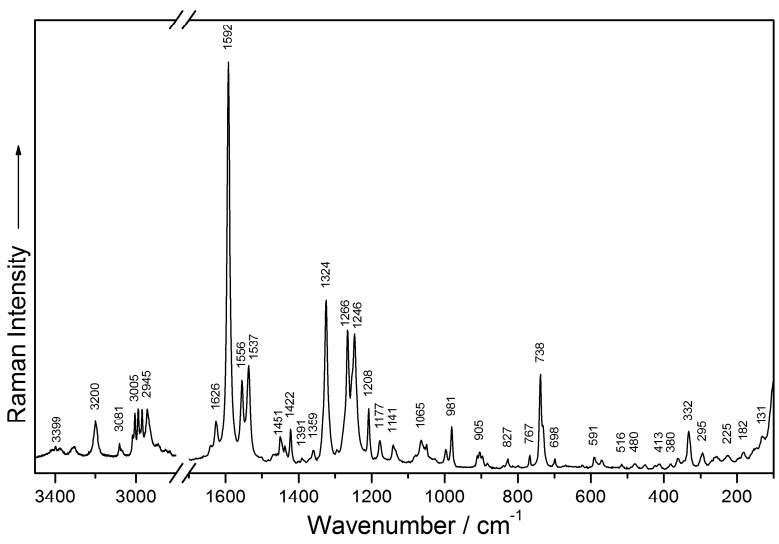

Figure 3. The Raman spectrum of metoclopramide hydrochloride powder

The spectrum is attributed to the protonated molecular form of metoclopramide. Because metoclopramide is available as hydrochloride and taking in consideration the pK_a value of 9.4, we suppose that metoclopramide crystallizes in the protonated molecular form. Moreover, the Raman spectrum of solid metoclopramide is dominated by the strong peak at 1592 cm^{-1}. This peak is also present at 1591 cm^{-1} as the strongest peak in the Raman spectra of metoclopramide aqueous solution in the 3-8 pH range (Fig. 4).

The experimental Raman wavenumbers, the corresponding calculated values together with the derived assignments for both, the protonated and neutral molecular forms of metoclopramide are listed in Table 2.

Table 2. Experimental and calculated wavenumbers (in cm^{-1}) of protonated and neutral molecular forms of metoclopramide, together with the corresponding assignments of the vibrational modes.

Protonated molecular form					**Neutral molecular form**		
calc. wavenumber.	**powder Raman**	**aqueous Raman**	**SERS prot.**	**Assignment**	**calc. wavenumber.**	**SERS neutral**	**Assignment**
115	131w			δ(C7H)			
147	145w			δ(C14H			
189	182w			δ(C16H)			
198	196vw			δ(N2H)			
236	225w			δ(C14H), δ(O7C7)			
256	257w			δ(C7H), δ(C10H)			
272	269vw			δ(C7H), δ(C10H)			
291	295w			δ(C16H), δ(C15H)			
302	303sh			δ(C10H), δ(C14H)			
325	332s	334m	337w	ip def(rg)	321	338w	ip def(rg)
352	363w			op def(rg)			
397	380w			δ(C10H), δ(C15H)			
415	413w	414vw		δ(C11H)			
439	424w		420w	δ(C3H), δ(C6H)			
449	452w	455vw	469w	δ(N2H)	459	461w	ip def(N12C13C14), ip def(N12C15C16)
459	480w			δ(N2H)			
511	516w			δ(C11H), δ(C10H)			
582	571w			δ(N9H)			
583	591w	593w	595w	δ(N9H)	583	597w	ip def(rg), δ(N2H)
612	624vw			ip def(rg), δ(N2H)			

662	698w			ν(C1Cl), ip def(rg)	660	665w	ν(C1Cl), ip def(rg)
669	732sh			op def(rg)			
722	738vs	738s	740s	breath(rg)	722	739s	breath(rg)
738	767w			op def(C5C8N9)			
790	798vw			δ(C3H), δ(C15H), δ(C16H)			
816	827w	832vw	839vw	δ(C13H), δ(C14H)	821	831m	δ(C13H), δ(C14H)
848	840vw			δ(C10H), δ(C11H)			
878	897w			δ(C14H), δ(C16H)			
909	905m	900vw		δ(C6H)			
911	911m			δ(C10H), δ(C11H), δ(C14H), δ(C16H)			
					978	934s	ν(rg), δ(C6H), δ(C7H), ip def (C4O7C7)
993	981s	986s	985w	ν(C15C16)	998	990m	ν(C15C16)
997	997m	1014vw	1018vw	ν(C13C14), ν(N12C13)	1038	1001m	ν(C13C14), ν(N12C13)
					1043	1031vw	δ(C3H), δ(C6H)
1035	1027vw			ν(C10C11), δ(N2H)			
1051	1049m	1057w	1053w	ν(N9C10), δ(C14H), δ(C11H)	1050	1053w	ν(C10C11)
1058	1065m			δ(C14H)	1081	1084vw	ν(N9C10), δ(N2H)
1134	1134sh			δ(C7H)			
1137	1141m	1152vw		ν(rg), δ(C7H)	1130	1130m	ν(rg), ν(C5C8), ν(N9C10)
					1164	1158vw	δ(C3H), δ(C6H), δ(C7H)
1173	1177m	1182m	1181w	δ(C3H), δ(C6H) δ(C7H)	1199	1179w	δ(C3H), δ(C6H), δ(C7H)
1203	1208s	1214s	1215	ν(C4O7), ν(C5C8),	1212	1212m	δ(N9H), δ(C10H),

			m	δ(C3H), δ(C6H), δ(C7H)			δ(C11H)
1245	1246vs	1259vs	1257vs	ν(C5C8), ν(N9H), δ(C10H), δ(C11H)			
1269	1266vs	1269vs	1269sh	ν(N9C10), δ(C14H), δ(C16H)	1271	1270vs	δ(C11H), δ(C10H), δ(N9H), δ(C13H), δ(C15H)
1282	1295w		1292sh	δ(C13H)	1289	1292vs	ν(rg), δ(C13H), δ(C15H)
1333	1324vs	1315vs	1321vs	ν(rg), δ(N2H)	1314	1313sh	ν(rg), δ(N2H)
1354	1359w			δ(C15H), δ(C13H)	1361	1366w	δ(C15H), δ(C13H)
1375	1371vw			δ(C10H9), δ(C11H)			
1398	1391w			δ(C14H)	1391	1393w	δ(C15H), δ(C16H)
1400	1401vw			δ(C16H)			
1414	1422s	1419m	1420m	ν(rg), δ(C7H)	1398	1413w	ν(rg), δ(C7H)
1438	1437m			δ(C10H), δ(C13H)			
1451	1445sh			δ(C11H)	1449	1447vw	δ(C7H)
1457	1451m	1457m	1455m	ν(rg), δ(C7H)			
1473	1470vw			δ(C7H)			
1497	1501vw			ν(rg)			
					1506	1511sh	δ(N9H), δ(C7H)
1536	1537vs	1543s	1539vs	ν(rg), δ(N9H)	1547	1544sh	ν(rg), δ(N2H)
1582	1556vs		1553sh	ν(rg), ν(C8O8), δ(N2H)	1589	1575sh	ν(rg), δ(N2H), ν(C8O8)
1606	1592vs	1591vs	1589vs	ν(rg), ν(C8O8), δ(N2H), δ(N9H), δ(N12H)	1624	1597vs	ν(rg), δ(N2H)

1629	1626w	1628sh	1650 w	δ(N2H)	1672	1648sh	ν(C8O8)
					2842	2855vs	ν(C11H), ν(C13H), ν(C15H)
2939	2940sh			ν(C7H)			
2953	2945 s	2957m	2946s	ν(C16H), ν(C14H)	2917	2928vs	ν(C14H)
2954	2955sh			ν(C16H), ν(C14H)			
2971	2968s		2979s	ν(C13H), ν(C15H)			
2976	2976sh			ν(C13H), ν(C15H), ν(C11H)			
3009	3005s	2999m	2994 m	ν(C10H)			
3015	3016m			ν(C13H), ν(C14H)			
3055	3068w			ν(C7H)			
3107	3081m	3084m	3077 m	ν(C3H)	3095	3073m	ν(C3H)
3124	3200s			ν(C6H)			
3465	3399m		3375s	ν(N2H)	3431	3380m	ν(N2H)

Abbreviations: w-weak, vw-very weak, m-medium, s-strong, vs-very strong, ip-in-plane, op-out-of-plane, def-deforming, ν-stretching, δ-bending, breath-breathing, rg-ring

For a reliable assignment of the Raman spectrum we based on the calculated wavenumbers considering the agreement with the experimental counterparts but also the intensity pattern of the experimental spectrum and the calculated Raman activities. Thus, from a total of 123 normal modes of the protonated metoclopramide, in Table 2 are reported only those calculated wavenumbers with an appreciable Raman activity and also with a correspondent experimental band in the Raman spectrum. All the omitted calculated normal modes have very low Raman activities.

According to the Handerson-Hasselbach equation[31] at these pH values metoclopramide exists in the protonated molecular form. This molecular species is easily water-soluble and the Raman spectrum in solution is unaffected in the pH range between 3 and 8. The assignments of the Raman bands of the protonated metoclopramide molecular form, present in aqueous solution, are shown in Table 2.

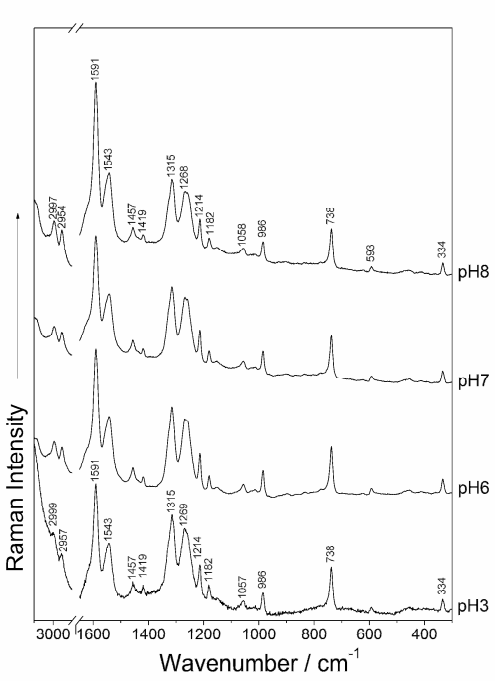

Figure 4. Raman spectra of 10^{-2} mol/l metoclopramide aqueous solutions in the 3-8 pH range.

By increasing the pH of the metoclopramide solution over 8 the metoclopramide solute molecules crystallize out, forming a suspension, and the metoclopramide Raman signal from the solution was too weak for recording the spectra. At pH values over 8, close to the pK_a value 9.4 of metoclopramide, according to the Handerson-Hasselbach equation the number of neutral metoclopramide molecules increases considerably. Consequently, this effect can be explained by a low solubility in water of the neutral metoclopramide molecular species.

Complementary to Raman spectroscopy, SERS spectroscopy monitors the molecules adsorbed to a metal surface without giving information about the bulk solution and represents a versatile tool for recording the vibrational spectrum in the pH domain with low solubility, due its high sensitivity - the potential of detection under the micromolar level. Fig. 5 presents the SERS spectra of metoclopramide in the 3-11 pH range. Small aliquots of 10^{-2} mol/l metoclopramide solution were added to the corresponding pH adjusted colloid, up to a final concentration of $5x10^{-6}$ mol/l.

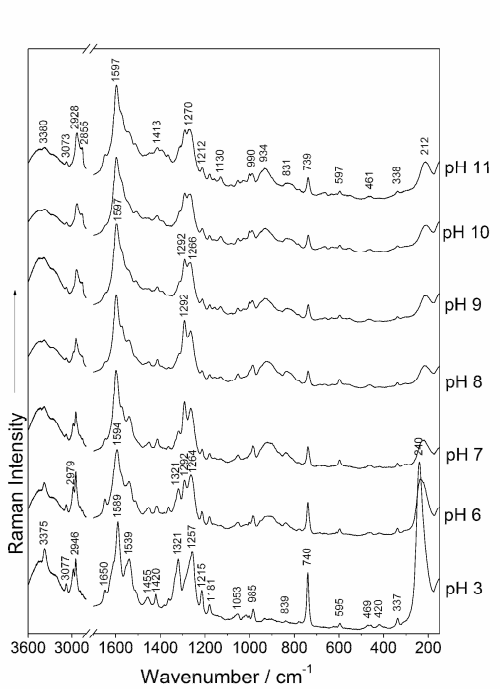

Figure 5. The SERS spectra of metoclopramide in the 3-11 pH range.

The SERS spectral table can be divided in three parts. Firstly, at pH 3 only protonated metoclopramide molecules are adsorbed to the silver surface, secondly in the 6-8 pH range on the silver surface coexist both molecular species, protonated and neutral, and thirdly the 9-11 pH range, where only neutral molecules are adsorbed to the silver surface.

Marker bands for the adsorbed protonated molecular species in the SERS spectra at pH 3 are the most intense bands at 1589, 1539, 1321 and 1257 cm^{-1}. The assignments of these bands are shown in Table 2.

The shape of the SERS spectrum at pH 6 is related to that of the SERS spectrum at pH 3 indicating the presence of mainly protonated metoclopramide molecular species adsorbed to the silver surface. Nevertheless, several changes in band positions and intensities compared to the SERS spectrum at pH 3 show the coexistence also of few neutral metoclopramide molecular species adsorbed to the silver surface. On passing in the spectra from pH 3 to pH 6, the characteristic bands for the protonated metoclopramide molecular species are blue-shifted to 1594 and 1264 cm^{-1} and being further shifted in the SERS spectra at higher pH values, whereas the bands at 1539 and 1321 cm^{-1} decrease in intensity and disappear totally in the SERS spectra at pH values over 9. Also at pH 6, a new peak appears at 1292 cm^{-1}, attributed to the neutral metoclopramide

molecules, being very intense in the SERS spectra at basic pH values. The attribution of the peak at 1292 cm^{-1} to the neutral molecular species is confirmed also by DFT calculations, this band being attributed to a ring stretching vibration (Table 2).

The coexistence of neutral molecular species with the protonated ones adsorbed to the silver surface already at pH 6 is not surprising, so far as several SERS studies[32-34] reported the adsorption to metal surfaces of unprotonated molecular species at pH values lower with two or more units than the pK_a value of the molecule.

At pH 7 and 8 the presence of neutral molecular species adsorbed to the silver surface is more evident. The peaks at 1539 and 1321 cm^{-1}, due to the protonated metoclopramide molecules decrease furthermore in intensity, whereas the peak at 1292 cm^{-1} attributed to the neutral metoclopramide molecular species increases in intensity, revealing that the number of neutral molecules adsorbed to the silver surface increased.

At pH values over 9, the lack of the characteristic bands of the protonated metoclopramide molecular species and the presence of the intense bands at 1597, 1292 and 1266 cm^{-1}, evidences the adsorption exclusively of neutral metoclopramide molecules to the silver surface.

In the high wavenumber region the passing from the protonated molecular form to the neutral one is evidenced by the shift of the peaks at 2979 and 2946 cm^{-1} due the protonated species to 2928 cm^{-1} with a shoulder at 2855 cm^{-1} for the neutral metoclopramide molecules. Also, with increasing pH, an intensity decrease tendency has been observed for the amide band at 3375 cm^{-1}.

In the SERS spectra recorded at acid pH values the metoclopramide-Ag stretching vibration is overlapped by the intense band at around 240 cm^{-1}, due to the stretching vibration $\nu(Ag\text{-}Cl^-)$ of the Cl^- anions adsorbed to the silver surface. However, the metoclopramide-Ag stretching band becomes evident at about 212 cm^{-1} in the SERS spectra recorded at basic pH values.

Theoretically, the interaction of metoclopramide with the silver surface can be established through the lone electron pairs of the N, O or Cl atoms of metoclopramide or through the π electrons of the ring.

Comparing the Raman spectrum at pH 3 from Fig. 4 with the corresponding SERS spectrum from Fig. 5 the band shapes of the two spectra are very close. All of the Raman bands can be retrieved in the SERS spectrum, blue or red shifted up to 10 cm^{-1} due to the interaction of metoclopramide molecules with the silver surface. Consequently, all Raman bands of metoclopramide appear enhanced in the SERS spectrum. Therefore, we conclude that all atoms of the molecule lie in the near vicinity of the silver surface, a necessary condition for observing SERS

enhancement, because of the strong gradient falling with distance of the electromagnetic field above the silver surface.[4,5]

On passing from the Raman spectra (Fig. 4) to the SERS spectra (Fig. 5), according to the surface selection rules[35,36] the normal modes, with a change in the polarizability component perpendicular to the surface are enhanced.

The ring breathing mode of metoclopramide at about 740 cm^{-1} usually gives rise to a strong Raman band independently of the protonation state of the molecule.[37] In the SERS spectrum at pH 3 the band at 740 cm^{-1} appears intense, therefore the adsorption of metoclopramide through the π electrons of the ring is less probable. However, the band at 740 cm^{-1} becomes weaker in the SERS spectra with increasing the pH. Therefore, according to the SERS selection rules, we suppose that the protonated metoclopramide molecular species are adsorbed in a perpendicular orientation of the skeletal ring to the silver surface, whereas the neutral ones are adsorbed in a tilted orientation to the silver surface. At pH values over 6 the unprotonated N12 atom can also be involved in the adsorption process leading to a more tilted orientation of the adsorbate.

REFERENCES - CHAPTER III

[1] Nicolae Leopold, Simona Cîntă-Pînzaru, László Szabó, **Daniela Ileşan**, Vasile Chiş, Onuc Cozar, Wolfgang Kiefer, Journal of Raman Spectroscopy, 41, 3, 248–255, 2010

[2] Damian G. *Talanta 2003; **60**: 923.*

[3] Moskovits M. *Rev. Mod. Phys.* 1985; ***57**:* 783.

[4] Otto A, Billmann J, Eickmans J, Ertuerk U, Pettenkofer C. *Surf. Sci.* 1984; **138**: 319.

[5] Otto A, Mrozek I, Grabhorn H, Akemann W*J. Phys.: Condens. Matter* 1992; **4**: 1143.

[6] Creighton JA, In *Spectroscopy of Surfaces*; Clark, R. J. H., Hester, R. E., Eds.; Wiley: New York, 1988; pp 37.

[7] Campion A, Kambhampati P. *Chem. Soc. Rev.* 1998; **27**: 241.

[8] Cotton TM. In *Spectroscopy of Surfaces*; Clark, R. J. H., Hester, R. E., Eds.; Wiley: New York, 1988; pp 91.

[9] Kneipp K, Kneipp H, Itzkan I, Dasari RR, Feld MS. *Chem. Rev.* 1999; **99**: 2957.

[10] Bell SEJ, Sirimuthu NMS. *Chemical Society Reviews* 2008; **37**: 1012.

[11] Cavalu S, Cîntă-Pînzaru S, Leopold N, Kiefer W. *Biopolymers – Biospectroscopy* 2001; **62**: 341.

[12] Cîntă-Pînzaru S, Cavalu S, Leopold N, Petry R, Kiefer W. *J. Mol. Struct.* 2001; **565-566**: 225.

[13] Szeghalmi AV, Leopold L, Pînzaru S, Chiş V, Silaghi-Dumitrescu I, Schmitt M, Popp J, Kiefer W. *J. Mol. Struct.* 2005; **735-736**: 103.

[14] Szeghalmi AV, Leopold L, Pînzaru S, Chiş V, Silaghi-Dumitrescu I, Schmitt M, Popp J. Kiefer W. *Biopolymers* 2005; **78**: 298.

[15] Cozar O, Leopold N, Jelic C, Chiş V, David L, Mocanu A, Tomoaia-Cotişel M. *J. Mol. Struct.* 2006; **788**: 1.

[16] Parr RG, Yang W. *Density-Functional Theory of Atoms and Molecules*, Oxford University Press, New York, 1989.

[17] Becke AD. *J. Chem. Phys.* 1993; **98**: 5648.

[18] Lee C, Yang W, Parr RG. *Phys. Rev. B* 1998; **37**: 785.

[19] Rauhut G, Pulay P. *J. Phys. Chem.* 1995; **99**: 3093.

[20] Scott AP, Radom L. *J. Phys. Chem.* 1996; **100**: 16502.

[21] Gellini C, Salvi PR, Vogel E. *J. Phys. Chem. A* 2000; **104**: 3110.

[22] Forth W, Henschler D, Rummel W, Starke K. *Allgemeine und spezielle Pharmakologie und Toxikologie*, Spektrum Akad. Verlag, 1998.

[23] Hansen B. *Acta Chem. Scand.* 1958; **12**: 324.

[24] Lee PC, Meisel D, *J. Phys. Chem.* 1982; **86**: 3391.

[25] M. J. Frisch, G. W. Trucks, H. B. Schlegel, G. E. Scuseria, M. A. Robb, J. R. Cheeseman, J. A. Montgomery, Jr., T. Vreven, K. N. Kudin, J. C. Burant, J. M. Millam, S. S. Iyengar, J. Tomasi, V. Barone, B. Mennucci, M. Cossi, G. Scalmani, N. Rega, G. A. Petersson, H. Nakatsuji, M. Hada, M. Ehara, K. Toyota, R. Fukuda, J. Hasegawa, M. Ishida, T. Nakajima, Y. Honda, O. Kitao, H. Nakai, M. Klene, X. Li, J. E. Knox, H. P. Hratchian, J. B. Cross, V. Bakken, C. Adamo, J. Jaramillo, R. Gomperts, R. E. Stratmann, O. Yazyev, A. J. Austin, R. Cammi, C. Pomelli, J. W. Ochterski, P. Y. Ayala, K. Morokuma, G. A. Voth, P. Salvador, J. J. Dannenberg, V. G. Zakrzewski, S. Dapprich, A. D. Daniels, M. C. Strain, O. Farkas, D. K. Malick, A. D. Rabuck, K. Raghavachari, J. B. Foresman, J. V. Ortiz, Q. Cui, A. G. Baboul, S. Clifford, J. Cioslowski, B. B. Stefanov, G. Liu, A. Liashenko, P. Piskorz, I. Komaromi, R. L. Martin, D. J. Fox, T. Keith, M. A. Al-Laham, C. Y. Peng, A. Nanayakkara, M. Challacombe, P. M. W. Gill, B. Johnson, W. Chen, M.

W. Wong, C. Gonzalez, and J. A. Pople, Gaussian 03, Revision E.01, Gaussian, Inc., Wallingford CT, 2004.

[26] Hehre WJ, Radom L, Schleyer PvR, Pople JA. *Ab Initio Molecular Orbital Theory*; John Wiley & Sons: New York, 1986.

[27] Flükiger P, Lühti HP, Portmann S, Weber J. *MOLEKEL 4.2*, Swiss Center for Scientific Computing, Manno (Switzerland), 2000-2002.

[28] Portmann S, Lühti HP. *Chimia* 2000; **54**: 766.

[29] Shin W., Chang T.S., Koo C.H. *Bul. Kor. Chem. Soc.* 1983; **4**: 123.

[30] Hall S.R., Allen F.H., Brown I.D. *Acta Cryst.* 1991; **A47:** 655.

[31] Atkins PW. *Physikalische Chemie*; VCH: Weinheim, 1987; 288.

[32] Giese B, Mc Naughton D. *J. Phys. Chem. B* 2002; **106**: 1461.

[33] Leopold N, Baena JR, Bolboacă M, Cozar O, Kiefer W, Lendl B. *Vib. Spectrosc.* 2004; **36**: 47.

[34] Leopold N, Cîntă-Pînzaru S, Baia M, Antonescu E, Cozar O, Kiefer W, Popp J. *Vib. Spectrosc.* 2005; **39**: 16.

[35] Creighton JA. *Surf. Sci.* 1983; **124**: 209.

[36] Moskovits M, Suh JS. *J. Phys. Chem.* 1984; **88**: 5526.

[37] Socrates G. *Infrared and Raman Characteristic Group Frequencies: Tables and Charts*; John Wiley & Sons, Ltd.: Chichester, UK, 2001.

CHAPTER IV
SPECTROSCOPIC STUDIES OF MANGANESE (II), COPPER (II) AND PALADIUM (II) COMPLEXES WITH DICLOFENAC AS LIGAND

Diclofenac sodium, (2-[2,6-dichlorophenilamino] phenylacetate) (L) and its complexes with transition metal are potent non-steroidal anti-inflammatory drugs, that have been used to alleviate the pain and edema associated with rheumatoid arthritis, osteoarthritis, spondylitis, and many other inflammatory conditions [1, 2].

The structure of diclofenac consists of a phenylacetic acid group, a secondary amino group, and a phenyl ring, both ortho position of which are occupied by chlorine atoms causing an angle of torsion between the two aromatic rings [3-5].

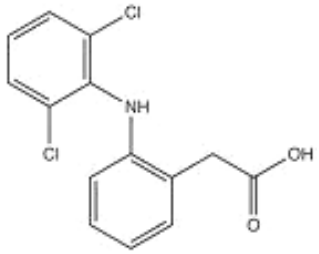

Fiure 1. Diclofenac structure

Some new diclofenac complexes: $[MnL_2(H_2O)]$ (**1**), $[PdL_2]$ (**2**) and $[CuL_2(H_2O)]$ (**3**), were synthesized by reaction of sodium diclofenac salt with $MnCl_2$, $K_2[PdCl_4]$ and $CuCl_2$ and characterized by FT-IR, UV-VIS and ESR spectroscopies.

2. EXPERIMENTAL

2.1 PHYSICAL-CHEMICAL MEASUREMENTS

The carbon, nitrogen, hydrogen, sulphur and oxygen were analyzed on Vario El device. Infrared spectra were recorded on a Perkin-Elmer FT- IR 1730 Spectrophotometer over KBr solid samples in 4000- 400 cm^{-1} range.

Electronic absorption spectra were recorded using a Jasco V-530 spectrophotometer. Powder EPR spectra of the synthesized complexes were measured at frequency of 9.56 GHz using standard ADANI Portable ESR spectrometer PS8400 equipment. The spectra were recorded at room temperature

2.2 SYNTHESIS OF THE COMPLEXES

The complexes were synthesized by reaction of the sodium acetate {2-[(2,6-dichlorofenil) amino] phenyl} with $MnCl_2 \cdot 4H_2O$, $K_2[PdCl_4]$, and $CuCl_2 \cdot 2H_2O$, according to the reactions:

$$MnCl_2 + 2NaL + H_2O \rightarrow [MnL_2(H_2O)] + 2NaCl$$

$$K_2[PdCl_4] + 2NaL + 2H_2O \rightarrow [PdL_2] \cdot 2H_2O + 2NaCl + 2KCl$$

$$2CuCl_2 + 4NaL + 4H_2O \rightarrow [CuL_2(H_2O)]_2 \cdot 2H_2O + 4NaCl$$

A 10 mL methanol solution was prepared containing 0.200 g $MnCl_2 \cdot 4H_2O$, 0.370 g $K_2[PdCl_4]$. Afterwards 0.170 g $CuCl_2 \cdot 2H_2O$ (1 mmol) were added under stirring, to a 10 mL of a methanol solution containing 0.64 g sodium Diclofenac (2 mmols).

The reaction mixture was stirred for 24 h. The solutions were cooled in refrigerator for 2 h and the solid (0.392 g $[MnL_2(H_2O)]$(**1**), 0.498 g $[PdL_2] \cdot 2H_2O$(**2**) and 0.897 g $[CuL_2(H_2O)]_2 \cdot 2H_2O$(**3**) respectively) were filtered, washed with cold methanol and ether, and dried in vacuo over silica gel.

3. RESULTS AND DISCUSSION

FT-IR SPECTROSCOPY

FT-IR spectra of the metallic complexes are compared in Fig.2 with the corresponding ligand. The FT-IR data for the diclofenac and its complexes are given in Table 2.

Because the carboxyl hydrogen is more acidic than the amino hydrogen, deprotonation occurs in the carboxylic group. This is confirmed by the FT-IR spectra of the **1-3** complexes comparatively with the ligand spectrum (Fig.2) showing the characteristic bands for the secondary amino group and for the coordinated carboxyl group.

In the $\nu(OH)_{water}$ region spectra of the (**1**) and (**3**) show a broad absorption at ~ 3500 cm^{-1} attributed to the presence of coordinated water.

Table 2. Characteristic vibrational bands (cm^{-1}).

	ν (OH)	ν_{as}	ν_s	ν(M-O)
L	3560 br;	1572 s	1402 s	-
1	3463	1577 s	1452 s	401 mw
2	3570 br	1577 s	1454 s	405 mw
3	3568 br;	1578 s	1452 s	403 m

The absence of large systematic shifts of the ν(NH) and δ(NH) bands in the spectra of these complexes compared with those of the ligand indicates that there is not interaction between the NH group and the metal ions.

The ν_{as}(COO) and ν_S(COO) bands of the complexes appear at 1577 cm^{-1} and 1452 cm^{-1} for (1), at 1577 cm^{-1} and 1454 cm^{-1} for (2), and at 1578 cm^{-1} and 1454 cm^{-1} for (3), respectively [6].

The difference Δ[Δ= ν_{as}(COO)- ν_S(COO)], is 125 cm^{-1} for (1), 123 cm^{-1} for (2) and 124 cm^{-1} for (3) has lower values than the one for sodium diclofenac (170 cm^{-1}), as expected for the bidentate bridging mode of carboxylate ligation [7,8].

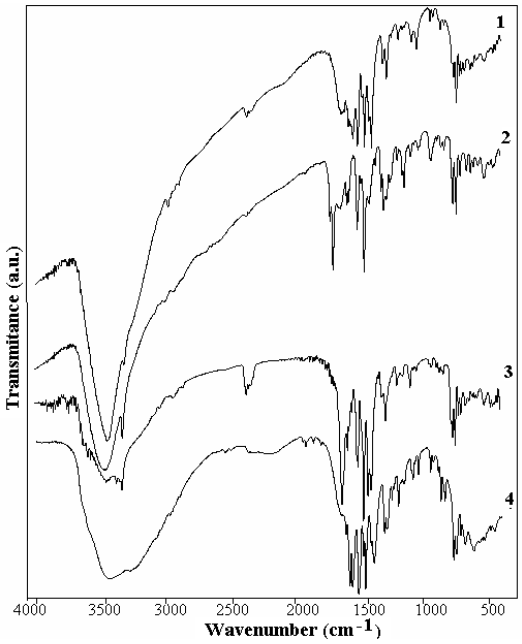

Figure 2. FT-IR spectra of the complexis and ligand

The strong band at 3388 cm^{-1} which appear in diclofenac, is assigned to the ν(NH) stretching motion and the broad band at 3260 cm^{-1} is taken to represent the ν(NO) mode, due to intramolecular hydrogen bonding [6].

The complexes (**1**) and (**3**) exhibit bands at 3563 and 3568 similarity of FT-IR spectra for ligand **L** and for complexes **1**, **2** and **3** shows that vibration bands are mainly due to the diclofenac structure. The shift of the ν_{as}(COO) antisymmetric and ν_{sym}(COO) stretching vibrations, the main band of the ligand, towards higher or lower energies in complexes indicates that the coordination increases the cohesion of the diclofenac ligand structure.[9,10]

The (**1**) and (**2**) complexes are mononuclear molecules and the complex (**3**) is a binuclear molecule. The two carboxylate groups from two ligands are in bidentate bridging mode for (**1**) and (**2**) complexes and the four carboxylate groups from four ligands are in bidentate bridging mode for complex (**3**). The square pyramid geometry with a water oxygen occupying one apical positions in (**1**) and (**3**) complexes respectively was established. For the complex (**2**) was established the square planar geometry.

ELECTRONIC SPECTROSCOPY

The electronic spectrum of the ligand presents three absorption bands at ν_1= 199 nm, ν_2= 209.5 nm, and ν_3= 282 nm, respectively. The ν_1 band is assigned to $\pi \rightarrow \pi^*$ transitions in conjugate organic systems, the ν_2 band is characteristic for $\pi \rightarrow \pi^*$ transitions in carboxylic group and the ν_3 band caused by the $n \rightarrow \pi^*$ transitions in aromatic system.

The electronic UV absorption spectra of the metal complexes are similar. The presence of different cations leads to a shift of the ν_2 bond towards higher (complex **3**) or lower (complexes **1** and **2**) energies in these spectra.

These shifts might be correlated with involvement of both oxygen atoms from the carboxylic groups of the ligand in the metal coordination, which caused a strengthening of the C-O bonds involved in the charge transfer processes for complex **3** and weakening of these bonds in the **1** and **2** complexes [11,12].

The UV absorption bands of the synthesized complexes are presented in Fig. 3 and confirm the bidentate character of the ligand.

UV spectra of the ligand and complexes are also very similar, evincing that the charge transfer inside the diclofenac structure is not significantly affected by coordination. However, the molar absorption coefficient of the ν_1 band, which is proportional to the number of the atoms, is almost twice greater in complexes than in the ligand. These values also indicate the existence of two **L** ligand units in the **1**, **2** and **3** complexes.

UV spectra show that transition metal ions co- ordination to the ligand intensifies the charge transfer into the diclofenac framework. The charge transfer into the C- O bonds is affected by the metal ions.

The complexes displayed in the VIS spectra other absorption bands (Fig. 4) which may be assigned to the d→d (IVCT) transitions or charge transfer transitions L→M (CT) due to the coordination of the oxygen atoms from ligand to the metallic cations [13].

In visible domain complex (**3**) exhibits a band at 709 nm attributed to a ligand field transition, and another one at 377 nm assigned to a charge-transfer from carbohydrate-oxygen atoms to the metal ion. These bands are typical for penta coordinated species with CuO_5 chromophore [14].

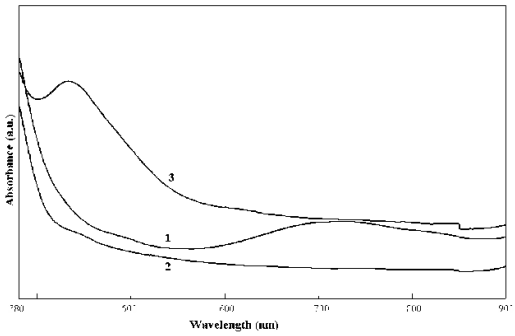

Fig. 3. UV spectra of the ***1****-[PdL2]·2H2O,****2*** *- [MnL2(H2O)],* ***3*** *- [CuL2(H2O)]2·2H2O and* ***4*** *- NaL·4H2O, in methanol (c=*10^{-5} *M).*

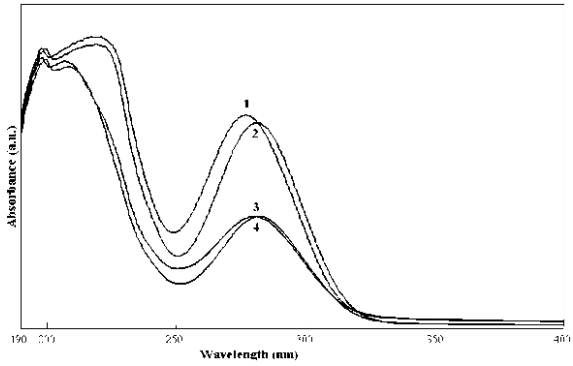

*Fig. 4. Visible spectra of the **1** - [CuL2(H2O)]2·2H2O, **2** - [MnL2(H2O)], **3** - [PdL2]·2H2O in methanol (c=10-3 M).*

ELECTRONIC SPIN RESONANCE SPECTROSCOPY

The polycrystalline powder ESR spectrum of $[MnL_2(H_2O)]$ complex, at room temperature is characterized by quasi-isotropic g tensor with the principal value (g=2.01) close to the spin only value [15]. The signal at $g \approx 4$ in the powder ESR spectrum of the Cu(II) complex suggests the presence of the dimeric species due to the dipol-dipol interaction between the metallic ions [16].

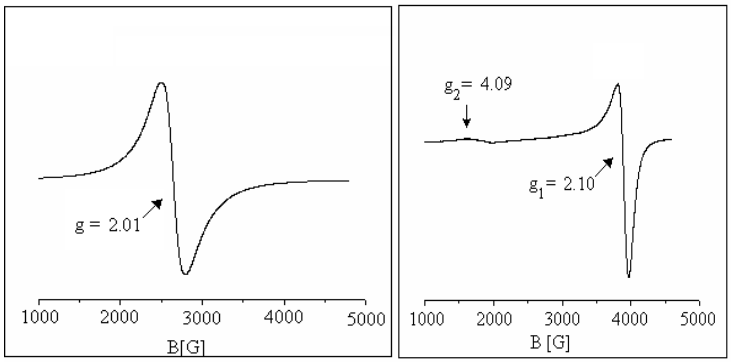

Fig. 5. Powder ESR spctrum of complex 1; powder ESR spctrum of complex.3.

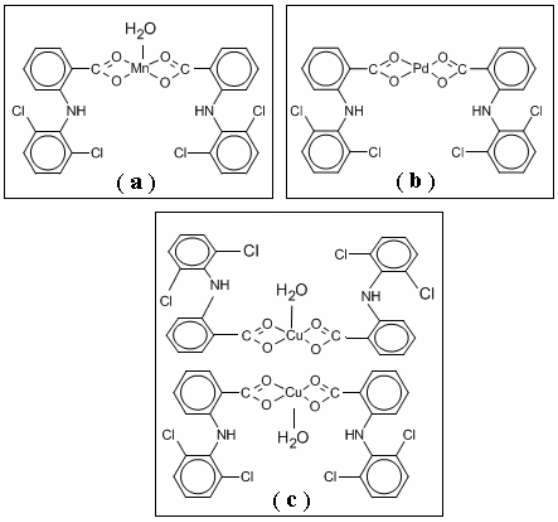

Figura. 6. Proposed structures for the $[MnL_2(H_2O)]$ (a), *PdL2],* (b) and *[CuL2(H2O)]2·2H2O*

REFERENCES – CHAPTER IV

[1]. D. Rusu, A. Marcu, M. Rusu, Daniela. Ilesan, L. David, Journal of Optoelectronics and advanced materials - Symposia, 2, 1, 94 – 97, 2010

[2] D. Kovala- Demertzi, S. K. Hadjikakou, M. A. Demertzis, Y. Deligiannanakis **69**, 223 (1998).

[3] D. Kovala- Demertzi, D. Mentzafos, A. Terzis, Polyhedron, **11**, 1361 (1993).

[4] D. Kovala- Demertzi, A. Theodorou, M.A. Demertzis, C. Raptopoluou, A. Terzis,in: Proceeding at the third GIPS, Senigalia, Italy, 1955.

[5] M. Tunçay, S. Çaliş, H. S. Kaş, M. T. Ercan, I. Peksoy, A. A. Hincal, Int. J. Pharmaeutics **195**, 179 (2000).

[6] K. Nakamoto, Infrared and Raman Spectra of Inorganic and Cordinaton Compounds, 4th ed. NewYork, Wiley, (1986).

[7] G. Socrates, Infrared and Raman Characteristic Group Frequencies: Tables and Charts, third edition,Wiley, Chichester , (2001).

[8] E. Prenesti, S. Berto, P. G. Daniele, Spectrochimica Acta **59**, 201 (2003).

[9] M. E. Palomo, M. P. Ballesteros, P. Frutos, Journal of Pharmaceutical and Biomedical Analysis **21**(1), 83 (1999).

[10] L. J. Bellamy, The Infra-red Spectra of Complex Molecules, Wiley, New York, 1975.

[11] W. Kemp, Organic Spectroscopy, 7th ed. London, MacMillan, 1984.

[12] A. Stanila, A. Marcu, D. Rusu, M. Rusu, L. David, Journal of Molecular Structure **834–836,** 364 (2007).

[13] A. B. P. Lever, Inorganic Electronic Spectroscopy, 2nd ed. New York, Elsevier, 1984.

[14] E. Prenesti, S. Berto, P. G. Daniele, Spectrochimica Acta, **59,** 201 (2003).

[15] F. Mabbs, D. Colisson, Electron Paramagnetic Resonance of d transition Metal Compounds, Elsevier, Amsterdam, 102, 1992.

[16] V. Noethig-Laslo, N. Pauli, Chemical Monthly, Springer Wien **128**, 1101 (1997).

GENERAL CONCLUSIONS

The Raman and SERS spectra of the protonated and the neutral metoclopramide molecular species were safely assigned, due to a good match between experimental and DFT calculated vibrational modes.

The Raman spectra of metoclopramide aqueous solutions were recorded only for the protonated molecular species in the 3-8 pH range, since the neutral metoclopramide species are low water soluble. SERS spectra of metoclopramide were recorded in the 3-11 pH range evidencing the protonated, neutral and the coexistence of both molecular species adsorbed to the silver surface. The neutral metoclopramide molecular species were evidenced on the silver surface even at pH 6.

All Raman bands of metoclopramide appear enhanced in the SERS spectra. The orientation of the protonated molecular species was deduced to be perpendicular to the silver surface, whereas the neutral molecular species are adsorbed in a tilted orientation.

Metal (II) complexes of diclofenac with interesting anti-inflammatory profiles have been prepared and studied by infrared, electronic and ESR spectroscopic methods.

The square pyramid geometry with a water oxygen occupying both apical positions in copper complex, one apical position in manganese complex and square plan geometry in palladium complex results from analytical and spectroscopic data.

The spectroscopic measurements results confirmed the metal-ligand bonds, the square-pyramidal symmetry of complexes (**1**) and (**3**) and the tetrahedral symmetry of complex (**2**).

Based on the chemical, and spectroscopic results the fallowing schematic structure of coordination for the synthesised complexes is proposed in Fig. 6.

ACKNOWLEDGMENT

My acknowledgements and my sincere appreciation to Professor David Leontin Ph.D., who guided me, supported me and generously shared some of this scientific knowledge during these years of postgraduate apprenticeship .

Also, I am grateful and thank the associate Prof. Dr. Nicolae Leopold and Dr. Vasile Chis as well as the research teams guided by them, for their support in making the experimental part and the opportunity to have access to valuable scientific work.

Finally, and not least, my thanks go to be beloved family, my children Hannelore, Alexandra and Robert, who have supported me and to my husband Marius and my father Gligore, who I've felt along the whole time and who encouraged me.

Cluj-Napoca,

20th of September 2013

Prof. Daniela-Florentina ILEŞAN